24th ABCM International Congress of Mechanical Engineering
December 3-8, 2017, Curitiba, PR, Brazil

# COBEM-2017-0328
# OPTIMIZATION OF A PLATE-FIN HEAT EXCHANGER BY DIFFERENTIAL EVOLUTION APPROACHES

**Douglas Mayer Rieger**
**Viviana Cocco Mariani**
Pontifícia Universidade Católica do Paraná, Programa de Pós-Graduação em Engenharia Mecânica, Pontifícia Universidade Católica do Paraná
douglasmr11@hotmail.com, viviana.mariani@pucpr.br

**Emerson Martim**
Programa de Graduação em Engenharia Química, PUCPR.
emerson.martim@pucpr.br

***Abstract.*** *In the present study, a single pass cross-flow plate-fin heat exchanger (PFHE) equipped with offset-strip fins was modelled and thermodynamically optimized. The method used for the modelling was the effectiveness-NTU and the program was MATLAB®. The process fluids are hot (fluid A) and cold air (fluid B). The optimization method used was the Differential Evolution (DE), which is based in the generation of an initial population (solutions) and subsequent processes of mutation, crossover and selection in order to create new generations, increase population diversity and prevent premature convergence. Posteriorly, DE was modified using two variants: Oppositional DE and Quasi-Oppositional DE. The optimized variables were the exchanger's length for each fluid,* $L_a$ *and* $L_b$*, the number of fin layers for A,* $N_a$*, the external height, H, thickness, t, frequency, n, and the lance length, l, of the fins. The main results were compared with previous literature using Genetic Algorithm (GA) and the Particle-Swarm Optimization (PSO) methods. The heat duty of the exchanger was fixed at 160 kW. Although the number of entropy generation ended up increasing (12,39% comparing to the AG), the fluids' pressures losses were significantly reduced (65.2% lower for A and 55.64% for B compared to the AG), and the transfer coefficients greatly increased (B increased by 96.31%).*

***Keywords:*** *Heat Exchanger, Optimization, Entropy, Differential Evolution.*

## 1. INTRODUCTION

The heat exchanger is the main industrial equipment used to perform heat transfer between two fluids. There are many applications of those: in air conditioning systems, refrigeration cycles (industrial and domestic), waste heat recovery, industrial scale sterilization, general chemical processing, aerospace, electronics, automobiles and many others. The fluids flow along the equipment and the hot transfer its energy to the cold through a solid wall constructed with a highly conductive material. The fluids can flow through the equipment parallelly (cocurrent), in countercurrent or in cross-flow. These different types of flow change some of the required correlations, grants different temperature profiles and allow different outlet conditions to be achieved (Lavine *et al.*, 2014; Moran *et al.*, 2013. Wen *et al.*, 2016).

The requirement for efficient, flexible, small and economic heat exchangers led to the development of the Plate Heat Exchangers (PHE). There are two classes of PFHs: the gasketed and plate-finned. The first is composed of packs of corrugated metal plates installed by gaskets that form flow channels for hot and cold fluids. They flow alternately between the plates, so that each stream of cold fluid is surrounded by two streams of hot fluid, enhancing the heat transfer (Gut, 2003).

The latter is a unison of the compact exchanger and the parallel plate one, consisting of a junction of flat plates called partition sheets with corrugations (wavy fins) welded between them. The fluids flow between the passages formed by the corrugations, which serve as a secondary heat exchanger surface area as well as mechanic support for the equipment's internal pressure. Thanks to their compactness, they are widely used in cryogenic gas separation processes and aerospace services (Wen *et al.*, 2016).

The shape of the fins can vary depending on the application between corrugated, triangular, square, perforated and others. The main employed types are illustrated in Fig. 1.

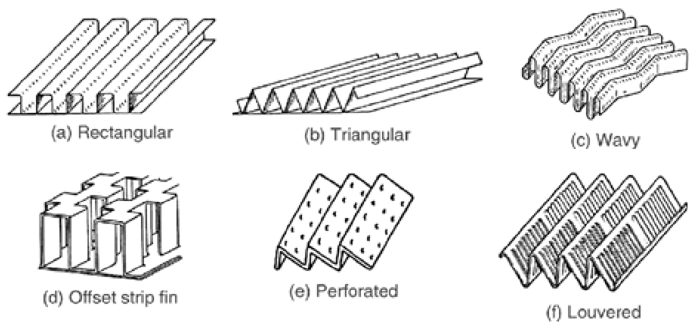


Figure 1. Fin types.

PFHE's are commonly used in gas-gas operations, capable of having area densities, heat transfer area per exchanger volume, up to 6000 $m^2/m^3$. The operation pressures are generally low, with the limit of 1000 kPa manometric. Permissible temperatures range from cryogenic uses to 1080 K, depending on the type of fin and plate material. Differing from the gasket PHEs, the contamination and leaking of process fluids is rare on this type of equipment (Kuppan, 2000).

It is important to note that these exchangers must not be used with excessively encrusting fluids, since the passage ducts are small and their cleaning is not simple. If there is significant risk of encrustation the wavy fins are recommended and the serrated ones must be avoided. Equipped with the right materials, the PFHEs can operate with almost absolute zero temperature fluids and pressures until around 14 MPa. Incidentally, though, the combination of pressure and temperature extremes should not be implemented (Kuppan, 2000).

These exchangers provide approximately 25 times more thermal exchange area than the shell and tube types (Kuppan, 2000). On Fig. 2 it is possible to visualize the plate-fin heat exchanger with wavy fins. On the left with cross-flow and on the right with countercurrent.

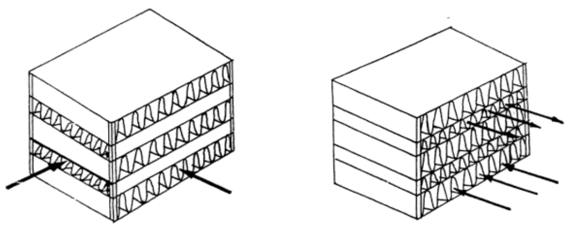

Figure 2. Plate-fin heat exchangers. Cross-flow (left) and countercurrent (right).

The thermodynamic optimization of a heat exchanger is based on the Second Law of Thermodynamics and can be referred as Entropy Generation Minimization (EGM), since the program aims to reduce the Number of Entropy Generation, a dimensionless parameter that represents the system's irreversibility. Greater values of this number translate as a loss of potential work or heat/mass transfer of the system (Rao & Patel, 2010).

Thus, the objective of the present work is to perform the analytic modelling of a cross-flow plate-fin (offset fin) heat exchanger and thermodynamically (minimize the entropy) optimize its physical dimensions by means of the Differential Evolution (DE) and its variants, the Oppositional DE and the Quasi-Oppositional DE.

## 2. METHODOLOGY

### 2.1 Heat Exchanger Modelling

In the present work, the mathematical modeling of a cross-flow plate-fin heat exchanger was carried out utilizing consolidated equations of the heat transfer literature. Then, the equipment was submitted to optimization by the Differential Evolution methods in a similar way as done by Mishra *et al.* (2009), who used the GA (Genetic Algorithm) and Rao & Patel (2010), who did it through the PSO (Particle Swarm Optimization). The program used was MATLAB®. Since only the inlet temperatures of the fluids were known, the effectiveness-NTU method was chosen.

The considerations made for the mathematical modeling were: steady state; same specification for the fins for both fluids; ideal gas behavior; constant heat transfer coefficients; constant free-flow and thermal exchange area and the number of fin layers for fluid B was considered one more than A. Also, knowing that during the flow throughout the equipment there is a change in the fluids' temperatures and, consequently, their thermophysical properties vary, a practical way to treat this variation is by using the average between the inlet and outlet temperatures for the determination of the fluids' properties. They are displayed in Tab. 1.

Table 1. Operation initial parameters.

| **Parameters** | **Unit** | **Fluid A (hot air)** | **Fluid B (cold air)** |
|---|---|---|---|
| Mass flow | kg/s | 0.8962 | 0.8296 |
| Inlet temperature | K | 513 | 277 |
| Average Temperature | K | 426.545 | 372.812 |
| Inlet pressure | Pa | $10^5$ | $10^5$ |
| Specific heat | J/kg.K | 1017.7 | 1006.54 |
| Specific mass | kg/m³ | 0.8196 | 1.2687 |
| Prandlt Number | - | 0.6878 | 0.7129 |
| Dynamic Viscosity | N.s/m² | 0.0000241 | 0.00001946 |
| Specific gas constant | J/kg.K | 286.986 | 286.986 |
| Exchanger's heat duty | kW | 160 | 160 |

The application of convective heat transfer correlations always counts on the use of dimensionless parameters. One of great importance is the Prandtl Number, $Pr$. It represents a relative measure between the thickness of the hydraulic and thermal boundary layers, classifying the fluids among their capacities of transferring momentum in relation to the energy transfer by diffusion. Depending only on thermophysical properties, it is also a tabulated numerical value. It is calculated as the ration of kinematic viscosity and thermal diffusivity (Lavine *et al.*, 2014) or can be expressed in terms of the dynamic viscosity, specific heat and thermal conductivity, as shown in Eq. (1).

$$Pr = \frac{\nu}{\alpha} = \frac{\mu . c_p}{k} \tag{1}$$

A frequently used property in the modeling of exchangers by the effectiveness method is the thermal capacity of the fluid, $C_i$. It is calculated by the Eq. (2) and measures the ease of promoting temperature variations in a given fluid. The higher its value, the more energy it needs to be transferred to change the temperature of such fluid.

$$C_i = \dot{m}_i . c_{p,i} \tag{2}$$

An energy balance can be applied for the hot and cold fluids, Eq. (3) and Eq. (4) respectively, in order to calculate the total heat transfer rate of the equipment.

$$\dot{q} = C_{hot} . (T_{in,hot} - T_{out,hot}) \tag{3}$$

$$\dot{q} = C_{cold} . (T_{out,cold} - T_{in,cold}) \tag{4}$$

Such rate can be related with the overall heat transfer coefficient, $U$, heat transfer area, $A_{ht}$, and logarithmic temperature difference, $\Delta T_{ML}$ by means of Eq. (5).

$$\dot{q} = U . A_{ht} . \Delta T_{ML} \tag{5}$$

The effectiveness of heat exchanger is expressed as the ratio of the actual transfer rate of the equipment to the maximum possible rate, Eq. (6).

$$\varepsilon = \frac{\dot{q}}{\dot{q}_{max}} \tag{6}$$

The maximum rate of heat transfer (in the denominator) can be reached when the hot fluid is cooled to the inlet temperature of the cold one, or when the cold is heated to the inlet temperature of the hot one. This temperature variation is the largest possible for the exchanger, as represented in Eq. (7).

$$\Delta T_{max} = T_{hot,in} - T_{cold,in} \tag{7}$$

As defined by the thermal capacity, the fluid with the smaller heat capacity suffers greater temperature variations. So, it is safe to assume that the maximum heat transfer rate shall occur with the fluid of minimum heat capacity value. Joining Eq. (6) and Eq. (7), the maximum heat transfer rate can be calculated by Eq. (8).

$$\dot{q}_{max} = \varepsilon . C_{min} . (T_{hot,in} - T_{cold,in}) \quad (8)$$

The value of effectiveness varies between 0 and 1, and can be calculated by means of graphs or empirical correlations. These vary with the type of flow and the number of passes in the equipment. For the exchanger in question (single pass, cross-flow and unmixed fluids), it is calculated by the Eq. (9).

$$\varepsilon = 1 - \left[\exp\left(\frac{1}{C_r}\right) NTU^{0,22} . \{\exp[-C_r . NTU^{0,78}] - 1\}\right] \quad (9)$$

All correlations of effectiveness are in the form of the Eq. (9) above, that is, they are a function of the parameter $C_r$ and $NTU$. The term $C_r$ is called capacitance ratio, which is the ratio of the minimum thermal capacity (the smaller value between two) by the maximum. Determined by Eq. (10).

$$C_r = \frac{C_{min}}{C_{max}} \quad (10)$$

The variable called $NTU$ is a dimensionless parameter called Number of Transfer Units. This variable is a measure of the efficiency of heat transfer systems, being calculated by Eq. (11).

$$NTU = \frac{U . A_{ht}}{C_{min}} \quad (11)$$

From the previous equation, it can be seen that the $NTU$ is related to the total transfer coefficient and the thermal exchange area. Therefore, it can be interpreted as a measure of the exchanger's size. High $NTU$ values represent a high heat transfer rate, as well as large equipment. Small values indicate that there are more opportunities for heat transfer if the length of the equipment is increased. Incidentally, it is not because a heat exchanger has an extremely high number of transfer units that it is optimized or providing the best service. The size of equipment that the $NTU$ value represents is a "thermal size", which only takes into account the heat transfer process.

Çengel & Ghajar (2012) demonstrate that the $NTU$ value has limits in which increases in size promote small variations in the fluids temperatures, providing minimal service at a great cost. The selection and dimensioning of heat exchangers should always be a compromise between thermal and hydraulic performance and the cost of the equipment.

The aspect of the exchanger can be seen in Fig. 3, where $L_i$ refers to the external length for each of fluid.

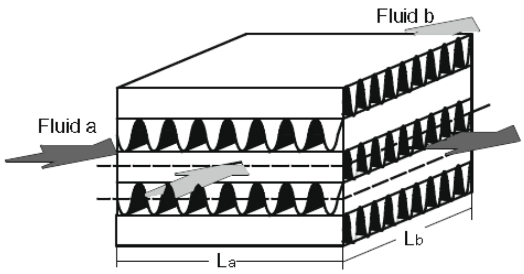


Figure 3. Plate-fin Heat Exchanger.

As for the offset-strip fins dimensions, $N_i$ is the number of layers (for each fluid), $H$ is the external height, $l$ the length, $h$ the internal height and $t$ is their thickness. The variable $n$ is a parameter used for the fin frequency calculation. These are all displayed in Fig. 4.

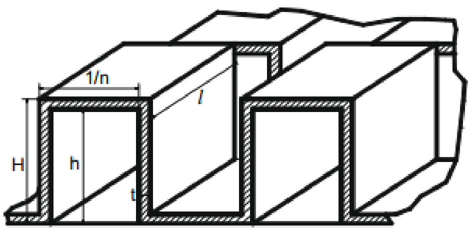


Figure 4. Offset fin dimensions.

The total heat transfer area, $A_{ht}$, in the previous equations is calculated by the sum of the individual heat transfer area for the fluids, which can be determined using Eq. (12) for fluid A and Eq. (13) for fluid B.

$$A_{ht,a} = L_a.L_b.N_a.[1 + 2n_a.(H_a - t_a)] \tag{12}$$

$$A_{ht,b} = L_a.L_b.N_b.[1 + 2n_b.(H_b - t_b)] \tag{13}$$

Another physical parameter of interest is the fin spacing, $s$. It can be calculated by the difference of the fin frequency and thickness, as in Eq. (14).

$$s = \frac{1}{(n_i)} - t_i \tag{14}$$

The flow area of the fluids is required for the determination of the hydrodynamic parameters and the exchanger pressure loss. In addition, it directly influences the heat transfer coefficients. The free flow $(ff)$ areas are calculated by Eq. (15) for fluid A and Eq. (16) for B.

$$A_{ff,a} = (H_a - t_a).(1 - n_a.t_a).L_b.N_a \tag{15}$$

$$A_{ff,b} = (H_b - t_b).(1 - n_b.t_b).L_a.N_b \tag{16}$$

One hydraulic parameter of extreme importance in convective heat transfer analysis is the dimensionless number of Reynolds, which classifies the fluid flow as laminar, transition or turbulent. It is also translated as the ratio between inertia and viscous forces on the fluid. It is calculated by means of Eq. (17).

$$Re_i = \frac{G_i.D_{h,i}}{A_{ff,i}.\mu_i} \tag{17}$$

Where the $G_i$ in is the mass flux (kg/m².s) of the fluid, determined by Eq. (18).

$$G_i = \frac{\dot{m}_i}{A_{ff,i}} \tag{18}$$

The term $D_{h,i}$ in Eq. (17) refers to the hydraulic diameter. For a circular pipe, the hydraulic diameter ends up being its own internal diameter. For the flat plates of a PFHE, $D_{h,i}$ is calculated by Eq. (19).

$$D_h = \frac{2.(s-t).(H-t)}{[s+(H-t)]+\frac{(H-t).t}{l}} \tag{19}$$

As fluids flow, the friction with surfaces promote loss of energy in the form of pressure decrease. The higher the pressure loss, more power is required for pumps and blowers to pump the fluids along the equipment, and the operational cost increase. In the dimensioning of a heat exchanger, the total pressure loss of the fluids is a determining factor of operation. It can be calculated by Eq. (20). Low velocities for the fluids help to avoid erosion, vibrations and reduce pressures drop (Çengel & Ghajar, 2012 and Lavine *et al.*, 2014).

$$\Delta P_i = \frac{4.f_i.L_i.G_i^2}{2.\rho_i.D_{h,i}} \tag{20}$$

The variable "$f$" in Eq. (20) is the Moody friction factor, another hydraulic dimensionless parameter. It can be obtained from empirical diagrams (Moody's Chart) or empirical correlations. It relates to the Reynolds number and the conditions of the flow surface. Its value increases with increasing surface roughness.

For laminar flow ($Re \le 1500$):

$$f = 8{,}12.(Re_i)^{-0{,}74}.\left(\frac{l_i}{D_{h,i}}\right)^{-0{,}41}.\left[\frac{s_i}{(H_i - t_i)}\right]^{-0{,}02} \tag{21}$$

For turbulent flow ($Re > 1500$):

$$f = 1{,}12.(Re_i)^{-0{,}36}.\left(\frac{l_i}{D_{h,i}}\right)^{-0{,}65}.\left(\frac{t_i}{D_{h,i}}\right)^{0{,}17} \tag{22}$$

The outlet pressure of the fluid can be easily determined with Eq. (23) once the pressure loss is known.

$$P_{i,out} = P_{i,in} - \Delta P_i \tag{24}$$

Going back to Eq. (10), the term $U$ refers the overall heat transfer coefficient. It is determined by the sum of the inverse of the system's thermal resistances, as indicated in Eq. (23).

$$U = \left[\frac{1}{(h.A_{ht})_a} + \frac{1}{(h.A_{ht})_b}\right]^{-1} \tag{25}$$

As in Eq. (23), it is noticed that only the convection resistances are being counted. This was considered because as the objective is to transfer as much heat as possible, the exchanger's material is highly conductive, making it so that the conduction resistance is very low and can be neglected. As explained in section 1, PFHEs are not used with fouling fluids, so that the thermal fouling resistances have also been disregarded.

The individual convective coefficients, $h_i$, in the denominator of Eq. (23), that are normally determined using the Nusselt number correlations, can alternatively written in terms of the Chilton-Colburn Analogy (or the Modified Reynolds Analogy), as presented in Eq. (24).

$$j_H = St.Pr^{2/3} \tag{26}$$

With $j$ being the Chilton-Colburn factor. According to Lavine *et al.* (2014), it represents a relationship between the coefficient of friction (hydrodynamic boundary layer), heat transfer coefficient (thermal boundary layer) and mass transfer coefficient (concentration boundary layer). The subscript "H" indicates "heat transfer", in order to differentiate it from the convective mass transfer analogy, $j_M$.

In Eq. (24), the term $St$ is called the Stanton Number (or modified Nusselt number), which can be determined by Eq. (25). This is another dimensionless parameter used in heat/mass transfer empirical correlations. It is calculated by the ratio of the Nusselt by the product of Reynolds and Prandtl numbers. Or, by expanding the dimensionless terms, it can be calculated using the ratio of the fluid's convection coefficient by the product of its specific mass, velocity and specific heat.

$$St = \frac{Nu}{Re.Pr} = \frac{h_i}{\rho_i.v_i.c_{p,i}} \tag{27}$$

The individual convective heat transfer coefficient, Eq. (26), can be determined by the substitution of Eq. (25) in Eq. (24).

$$h_i = j_{H,i}.\frac{\dot{m}_i}{Aff_i}.c_{p,i}.Pr^{-2/3}{}_i \tag{28}$$

The Chilton-Colburn factor value depends on the type of flow, being determined by empirical correlations. It is a function of the Reynolds number and the physical dimensions of the equipment, as indicated in the following equations.

For laminar regime ($Re \leq 1500$):

$$j = 0{,}53.(Re_i)^{-0{,}50}.\left(\frac{l_i}{D_{h,i}}\right)^{-0{,}15}.\left[\frac{s_i}{(H_i - t_i)}\right]^{-0{,}14} \tag{29}$$

For turbulent regime ($Re > 1500$):

$$j = 0{,}21.(Re_i)^{-0{,}4}.\left(\frac{l_i}{D_{h,i}}\right)^{-0{,}24}.\left(\frac{t_i}{D_{h,i}}\right)^{0{,}02} \tag{30}$$

From the previous definitions for the transfer coefficients and transfer areas, the value of NTU can ultimately be determined as Eq. (29).

$$NTU = \left\{C_{min}.\left[\frac{1}{(j_a.\dot{m}_a.c_{p,a}.Pr^{-2/3}{}_a)}\frac{A_{ff\,a}}{A_{ht,a}} + \frac{1}{(j_b.\dot{m}_b.c_{p,b}.Pr^{-2/3}{}_b)}\frac{A_{ff\,b}}{A_{ht,b}}\right]\right\}^{-1} \tag{31}$$

The fluid's outlet temperatures can be calculated by applying an energy balance to each fluid, or utilizing the maximum heat transfer multiplied by the effectiveness, which grants the real heat transfer rate. Isolating the term $T_{i,out}$ results in Eq. (30) and Eq. (31) for fluids A and B respectively.

$$T_{a,out} = T_{a,in} - \frac{\varepsilon . C_{min} . (T_{a,in} - T_{b,in})}{C_a} \tag{32}$$

$$T_{b,out} = T_{b,in} + \frac{\varepsilon . C_{min} . (T_{a,in} - T_{b,in})}{C_b} \tag{33}$$

Knowing the output conditions of the equipment, it is possible to calculate the entropy change for each fluid and the total rate of entropy generation. As described in Bejan (1977), Eq. (32) is for fluid A and Eq. (33) for B.

$$\Delta S_a = c_{p,a} . ln \frac{T_{a,2}}{T_{a,1}} - R_a . ln \frac{P_{a,2}}{P_{a,1}} \tag{34}$$

$$\Delta S_b = c_{p,b} . ln \frac{T_{b,2}}{T_{b,1}} - R_b . ln \frac{P_{b,2}}{P_{b,1}} \tag{35}$$

The total rate of entropy is nothing more than the sum of the individual rates, as presented in Eq. (34).

$$\dot{S} = \dot{m_a} . \Delta S_a + \dot{m_b} . \Delta S_b \tag{36}$$

Finally, the number of entropy generation, the objective function, is determined by the total entropy rate and the maximum heat capacity, Eq. (35).

$$N_s = \frac{\dot{S}}{C_{max}} \tag{37}$$

Substituting equations 30 to 34 in 35 allows to rewrite the number of entropy generation in the format of Eq. (36) like performed by Mishra *et al.* (2009).

$$N_s = \frac{C_a}{C_{max}} . \left[ ln \left\{ 1 - \varepsilon . \frac{C_{min}}{C_a} . \left( 1 - \frac{T_{b,1}}{T_{a,1}} \right) \right\} - \frac{R_a}{c_{p.a}} . ln \left( 1 - \frac{\Delta P_a}{P_{a,1}} \right) \right] + \frac{C_b}{C_{max}} . \left[ ln \left\{ 1 + \varepsilon . \frac{C_{min}}{C_b} . \left( \frac{T_{a,1}}{T_{b,1}} - 1 \right) \right\} - \frac{R_b}{c_{p.b}} . ln \left( 1 - \frac{\Delta P_b}{P_{b,1}} \right) \right] \tag{38}$$

After the modeling of the equipment, the physical dimensions were submitted to optimization. The results were applied in the previous equations to determine the parameters of the exchanger and evaluate its performance.

### 2.2 Numerical Verification

After the exchanger's modelling, the numerical verification was performed, that is, the optimized data (physical parameters of the heat exchanger) of Mishra *et al.* (2009) were applied in order to obtain the same results for the heat rate (fixed value) and number of entropy generated. The detailed results of the verification are given in section 3.

### 2.3 Optimization

In this work, the method of optimization used was the Differential Evolution (DE), which was developed by Storn & Price (1995). ED is a stochastic method based on evolutionary principles. An initial population is generated randomly and mutation, crossover and selection procedures are applied in order to reach vectors that fit into a previously established optimum. It presents as advantages: hardly get stuck in local optimums (since it looks for the optimum in different regions of the search space); efficient to optimize discontinuous functions, as no information on the derivative of the function is required; the input and output parameters can be manipulated as real numbers (floating points), facilitating computational processing; effective operation even with small populations and is a good local optimizer, since the different values generated from a population become infinitesimal (Oliveira, 2006).

Mutation is the generation of a new vector from the weighted sum of the difference of two random vectors with a third one. This weighting is performed by means of a mutation factor, $F$. This value can be any number within the interval [0,2] (Rahnamayan *et al.*, 2008). Storm & Price (1995) suggest the use of 0.8 as the value of $F$. A technique called "dither" is used to significantly improve the convergence (depending on the objective function). It consists on making the mutation factor vary between 0.5 and 1.0 for each iteration within one run of the code.

The crossover of vectors is the operation of generating new solutions through operations between existing vectors. This technique is used to increase population diversity. A vector called "donor" shares its parameters with the ones of the "target" in order to generate the "trial" vector. This vector, therefore, inherits data from both, and the degree of similarity with the generating vectors depends on the probability of crossing, $C_r$. When $C_r$ is null, all inherited properties come from the target. When $C_r$ is equal to the unity, all data comes from the donor. The value of the crossing factor, therefore, varies between 0 and 1 (Oliveira, 2006 and Storn & Price, 1995).

Selection is the last stage of ED. In this step, it is decided which vector will become a member of the next generation. The target and trial vectors' suitability to the objective function are compared and the one with the greatest qualification for the optimum (generates the least amount of entropy) advances (Rahnamayan *et al.*, 2008).

Evolutionary optimization methods start from initial solutions (populations) that are continuously improved to an optimum that fits previously described conditions. When no information about the solution is readily known, the first vector is created from random assumptions. Since this is a random choice, computational time may be higher for different rounds of optimization. One way to reduce the processing length (which is translated as the distance from the initial vector to the solution one) is by the use of the "oppositional vectors". Probability theory confirms that 50% of the time the opposing vector is closer to the optimal solution than the initial. Therefore, it is perceived that checking the opposite is helpful for convergence speed. This principle is what granted the development of DE's variations Oppositional and Quasi-Oppositional. These two other methods are rather similar with classic ED, having small variations to account for the "Opposite Vectors" generation and comparison. More details about the optimization schemes are indicated in Storn & Price (1995) and Rahnamayan *et al.* (2008).

The seven variables submitted to the optimization were the exchanger's physical dimensions. Their significance and constraints are presented in Tab. 2.

Table 2. Variables' constraints.

| **Variable** | **Unit** | **Constraint** |
|---|---|---|
| Exchanger's outside length for fluid A, $L_a$ | m | $0.1 \leq L_a \leq 1.0$ |
| Outside length for fluid B, $L_b$ | m | $0.1 \leq L_b \leq 1.0$ |
| Fin external height, $H$ | m | $0.002 \leq H \leq 0.01$ |
| Fin frequency, $n$ | $m^{-1}$ | $100 \leq n \leq 1000$ |
| Fin thickness, $t$ | m | $0.0001 \leq t \leq 0.0002$ |
| Fin length, $l$ | m | $0.001 \leq l \leq 0.01$ |
| Number of fin layers, $N_a$ | m | $1 \leq N_a \leq 10$ |

## 3. RESULTS AND DISCUSSION

### 3.1 Numerical Verification

The variables that could be verified were only the mass flows. The convective heat transfer coefficient of fluid A, the pressure losses and the entropy generation rate were close to the expected results. The heat transfer rate, B's coefficient and the number of entropy, however, were far from the suggested values. A similar value for the entropy generation number could be achieved only when the total heat transfer rate would extrapolate the fixed value of 160 kW.

One of the reasons for this discrepancy is the use of few significant digits in the results and properties presented by Mishra *et al.* (2009). Although it may seem not so relevant in the final result, the use of more decimals proved crucial for the acquisition of results in the use of differential evolution. The validation could not be fully achieved, but the values found are sufficient to proceed with the code and modeling performed.

### 3.2 Mathematical Modelling and Optimization

The results of the application of the three optimization methods are displayed in Tab. 3, which compares the previous works on which this paper was based on. It is possible to verify the values for the physical dimensions in each case as well as the main parameters of the heat exchanger.

The mutation factor ($F$) was varied between 0.5 and 1.0 (dither) by means of the function $F = 1/\left[1 + e^{\left(-2.\frac{iter}{1000}\right)}\right]$ with $iter$ being the number of the iteration and $C_r$ (crossing probability) was 0.9, as suggested by Storn & Price (1995). The optimization strategy of number 7 (binomial) was used. The population size ($NP$) was assumed to be 40 and 5000 iterations were performed for each of the 30 runs. For the oppositional methods, the jumping factor $J_r$ was 0.3, as suggested by Rahnamayan *et al.* (2008). Matlab® was the program used for the implementation of the methods. According to Storn and Price (1995), empirical practices have shown that increasing the NP value beyond 40 does not provide substantial improvements to convergence, hence the reason for choosing such value.

Table 3. Comparative of the modelling results.

| Variable | Unit | GA | PSO | ED | EDO | EDQO |
|---|---|---|---|---|---|---|
| $L_a$ | m | 0.994 | 0,925 | 1.00000 | 1.00000 | 1.00000 |
| $L_b$ | m | 0.887 | 0.996 | 0.87899 | 0.87899 | 0.87899 |
| $H$ | m | 0.00953 | 0.0098 | 0.01000 | 0.01000 | 0.01000 |
| $n$ | m | 534.9 | 442.9 | 442.3608 | 442.3608 | 442.3608 |
| $t$ | m | 0.000146 | 0.0001 | 0.000100 | 0.000100 | 0.000100 |
| $l$ | m | 0.0063 | 0.0098 | 0.010000 | 0.010000 | 0.010000 |
| $N_a$ | - | 8.00 | 10.00 | 10.00 | 9.9999 | 10.00 |
| $N_b$ | - | 9.00 | 11.00 | 11.00 | 10.9999 | 11.00 |
| $\dot{q}$ | kW | 159.99 | 159.99 | 159.9899 | 159.990 | 159.990 |
| $h_A$ | W/m².K | 797.00 | 1131.7 | 811.3000 | 811.3000 | 811.3000 |
| $h_B$ | W/m².K | 817.00 | 844.00 | 1603.847 | 1603.847 | 1603.847 |
| $G_A$ | kg/m².s | 14.59 | 11.71 | 10.7754 | 10.7754 | 10.7754 |
| $G_B$ | kg/m².s | 10.72 | 9.79 | 7.97058 | 7.97058 | 7.97058 |
| $\Delta P_A$ | N/m² | 5287.70 | 3331.3 | 1839.776 | 1839.776 | 1839.776 |
| $\Delta P_B$ | N/m² | 2216.90 | 1834.5 | 983.452 | 983.452 | 983.452 |
| $\dot{S}$ | W/K | 77.47 | 64.86 | 64.9243 | 64.9243 | 64.9243 |
| $N_S$ | - | 0.063332 | 0.053028 | 0.071183 | 0.071183 | 0.071183 |
| Earliest Convergence Iteration | - | - | - | 2600 | 2300 | 1900 |

From Tab. 3 it can be seen that all three methods granted the same result. This suggests that the classic ED already reached the optimum, and the variants provided nothing more than faster convergence over the iterations. Incidentally, QODE was the fastest to reach the optimum, achieving it on iteration 1900. While ODE was the second best, on 2300 and ED on 2600. This is in accordance to what explained by Rahnamayan *et al.* (2008).

The resulting dimensions of the exchanger much resembled PSO's values. The objective function, $N_S$ , presented, for the same total heat transfer rate, a value 12.39% higher than what found by the GA. Although the exchanger in question has a higher generation of entropy than the previously modeled ones, other important parameters for the operation of the equipment have been improved. The generation of entropy is only one approach for verifying the efficiency of the exchanger. While the convective heat transfer coefficient for fluid A had a slight decreased, B's increased by 96.31% compared to GA and 90.03% to PSO. Higher coefficients denote higher rates of heat transfer, improving the performance of the exchanger.

The variables that presented the best results were the pressure drops. For fluid A there were reductions of 65.21% in comparison to GA and 44.77% in relation to PSO. For B, reductions of 55.64% were obtained in relation to the GA and 46.39% in the PSO. The pressure drop is directly linked to the required power of pumps and blowers to move fluids into the exchanger. In addition, it is a limiting parameter of design that, depending on the magnitude of its value, makes it inviable to design a heat exchanger. In this way, lower pressure drop grants better operation and greatly reduces the operational cost. A graphical comparison between the pressure drops for fluids A and B within the three studies (GA, PSO and ED) is presented in Figure 5.

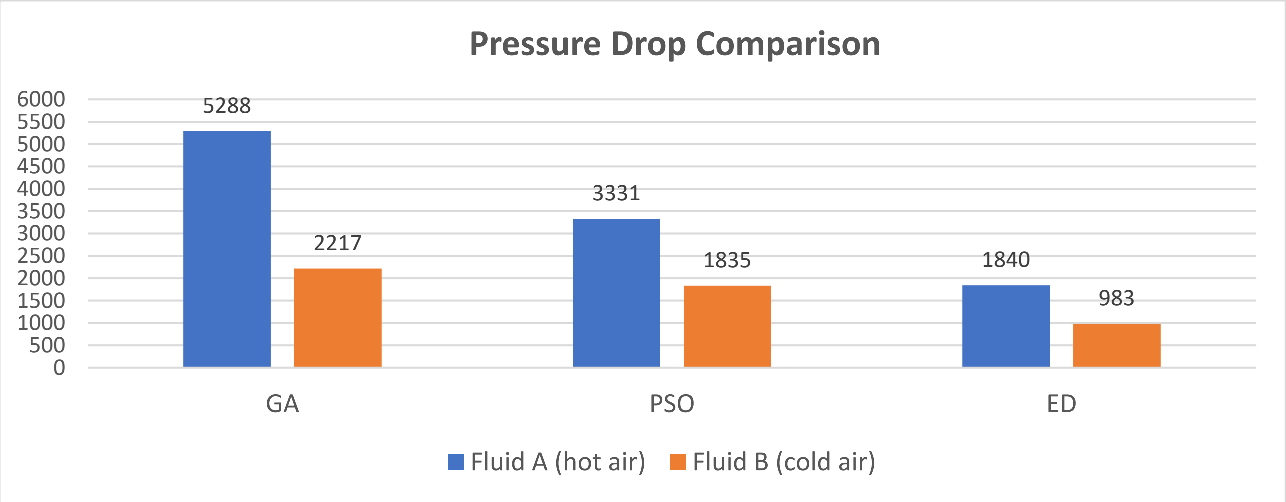


Figure 5 - Pressure drop comparison between the three studies.

It can be seen that the increase in external height and fin length promoted an enhancement in the overall coefficient of heat transfer due to the large improvement of the individual cold air convective coefficient. This raise is justified by the increase of the thermal exchange area, which is also reflected in the reduction of the mass flows. One way to check if the trade-off between the largest number of entropy and the lower pressure drop is worth is by calculating the cost of operating the equipment.

In Tab. 4 some other parameters of the exchanger, which were not presented by the other authors, can be visualized. They are useful in analyzing the equipment's performance. It can be seen that the flow of fluids was laminar (which is expected from the compact heat exchangers). In addition, the NTU of 7.1208 is a considerably high value, reflecting the most robust exchanger that was obtained. The equipment had an effectiveness of 80,805%. The friction and Colburn factors were also displayed for verification.

Table 4. Exchanger Thermal parameters.

| **Variable** | **Unit** | **ED, EDO, EDQO** |
|---|---|---|
| U | W/m². K | 33.1644 |
| NTU | - | 7.1208 |
| $\varepsilon$ | - | 0.80805 |
| $Re_A$ | - | 1500.00 |
| $Re_B$ | - | 1225.70 |
| $f_A$ | - | 0.02179 |
| $f_B$ | - | 0.015903 |
| $j_A$ | - | 0.0080806 |
| $j_B$ | - | 0.015903 |

## 4. CONCLUSIONS

In the present study, the design and thermodynamic optimization of a cross-flow plate-fin heat exchanger (offset fin type) with hot and cold air was carried out. The seven major physical dimensions of the exchanger and fins were optimized within specified constraints by Classic, Oppositional and Quasi-Oppositional Differential Evolution methods. Their resulting values were applied in the mathematical modeling of the exchanger in order to calculate the heat transfer parameters and evaluate the exchanger's efficiency. The results were compared with Mishra *et al.* (2009) and Rao & Patel (2010), who optimized the same type of equipment.

The three methods granted the same results, varying only on the convergence speed, with QODE being the fastest and ED the slowest. Several of the dimensions found by the EDs were larger than the literature, resulting in a larger heat transfer area and a much higher convective coefficient for the cold fluid. Such result is also translated as the high NTU obtained.

The Number of Entropy Generation was 12.39% higher than that found by GA, but the pressure losses reduced 65.206% for A and 55.64% for B. Lower pressure loss is a very positive factor for the operation since this parameter is a limiting factor for the design of heat exchangers and reduces the power of pumps and fans required to transfer fluids throughout the equipment, consequentially reducing the equipment's operational cost.

Despite generating more entropy, the equipment dimensioned by ED promotes benefits in terms of flow and transfer coefficients, which are also parameters of great importance in heat exchangers. The entropy analysis is a thermodynamic approach to equipment performance, which does not make design unfeasible, especially since the resulting entropy increase was just slightly higher from of the previous literature.

The ED methods proved to be very efficient for the optimization of heat transfer problems due to its computational agility and ease of implementation. The results obtained by the program were satisfactory and met the requirements of the project.

## 5. ACKNOLEDGEMENTS

The authors would like to thank National Council of Scientific and Technologic Development of Brazil - CNPq (grants: 405101/2016/3, and 303906/2015-4-PQ) for the support of this work.

## 6. REFERENCES

Bejan, A., 1977. The concept of irreversibility in heat exchanger design: counterflow heat exchangers for gas-to-gas applications. ASME Journal of Heat Transfer, Vol. 99, p. 374–380.

Çengel, Y. A. & Ghajar, A. J., 2012. Transferência de calor e massa: uma abordagem prática. 4ª Edição. Porto Alegre: Mcgraw-Hill Brasil Editora.

Gut, J. A. W., 2003. Configurações ótimas para trocadores de calor a placas. São Paulo. PhD thesis, University of São Paulo.

Kuppan, T., 2000. Heat exchanger design handbook. 1ª Edução. India: CRC Press.

Lavine, A. S., Dewitt, D. P., Incropera, F. P. & Bergman, T. L., 2014. Fundamentos da Transferência de Calor e Massa. 7ª Ed. Rio de Janeiro: LTC Editora.

Mishra M., Das, P. K. & Sarangi, S., 2009. Second law based optimization of cross plate-fin heat exchanger design using genetic algorithm. Applied Thermal Engineering. India, vol. 29, p. 2983-2989.

Moran, M. J., Shapiro, H. N., Boettner, D. D. & Bailei, M. B., 2013. Principles of Engineering Thermodynamics. 7ª Ed: LTC Editora. Rio de Janeiro.

Oliveira, G. T. S., 2006. Estudo e Aplicações da Evolução Diferencial. Uberlandia. Master dissertation, Federal University of Uberlandia.

Rahnamayan, S., Tizhoosh, H. R., & Salama, M. M. A., 2008. Opposition-Based Differential Evolution. Ontario, Canada. IEEE Transactions on Evolutionary Computation, vol. 12, n.1, p. 64-79.

Rao, R. V; Patel, V. K., 2010. Thermodynamic optimization of cross flow plate-fin heat exchanger using a particle swarm optimization algorithm. International Journal of Thermal Sciences. India, Vol. 49, p. 1712-1721.

Storn, R. & Price, K., 1995. Differential Evolution – a simple and efficient adaptive scheme for global optimization over continuous spaces. München.

Wen, Jian; Yang, Huizhu; Tong, Xin; Wang, Simin; Li, Yanzhong., 2015. Optimization investigation on configuration parameters of serrated fin in plate-fin heat exchanger using genetic algorithm. International Journal of Thermal Sciences. China, 101, p. 116-125.

## 7. RESPONSIBILITY NOTICE

Rieger, Mariani and Martim are the only responsible for the printed material included in this paper.